IEEE Access
Multidisciplinary | Rapid Review | Open Access Journal

Received 8 January 2024, accepted 1 February 2024, date of publication 5 February 2024, date of current version 12 February 2024.

Digital Object Identifier 10.1109/ACCESS.2024.3362296

RESEARCH ARTICLE

Compact Multiband Handset Antenna Design for Covering 5G Frequency Bands

MOHAMED LAMINE SEDDIKI[1], MOURAD NEDIL[1], (Senior Member, IEEE), SOUFIANE TEBACHE[2], AND SAIF EDDINE HADJI[1]

[1]LRTCS University of Quebec, Engineering School, Université du Québec en Abitibi-Témiscamingue (UQAT), Rouyn-Noranda, QC J9P 1Y3, Canada
[2]Ecole Nationale Polytechnique (ENP), El Harrach 16200, Algeria

Corresponding author: Mohamed Lamine Seddiki (mohamedlamine.seddiki@uqat.ca)

ABSTRACT New multiband antenna array structure with high gain is proposed for 5G communication handheld systems (700MHz/3.5 GHz and 28/38 GHz). The designed structure is proposed using a combination of sub-6GHz and mm-Wave antenna arrays. The antenna is based on S-shaped strip etched on the top side to operate at 700 MHz. On the other hand, the 3.5GHz band is generated by coupling a meander line to an inverted-C strip on the bottom side. Finally, the mm-Wave antenna array is based on four quadrupole elements with a 1:4 microstrip power divider. This configuration ensures that all four quadrupole antennas receive in-phase feeding power. Obtained results confirm that the designed antenna array achieves gains of 4.6 dBi, 10.5 dBi, at sub-6 GHz and mm-Wave band, respectively. Owing to its simplicity and compactness, the proposed handset antenna is a good candidate for 5G multiband applications.

INDEX TERMS Multiband, handset, 5G, mm-wave antenna, sub-6 GHz.

I. INTRODUCTION

The sub-6 GHz as well as the millimeter-wave (mm-Wave) bands are considered key technologies for fifth-generation (5G) wireless networks to overcome drawbacks related notably to power attenuation in the surrounding environment and aiming to achieve high throughput, low latency and low transmission power [1]. In this area, path loss is generally associated to mm-Wave band compared to low frequency band. Mostly, antenna arrays with increased gain and wider angular coverage are one of the most promising solutions to deal with path loss issue [1], [2], [3], [4]. In fact, the Sub-6GHz (700 MHz/3.5 GHz) band provides a better coverage with lower propagation losses in a heterogeneous environment. Besides, particular interest is still raised by scientific community jointly with industrial world to embed mm-wave radiators in small mobile devices. Consequently, the combination of sub-6 GHz and mm-Wave antenna design in the same shared volume is foreseen to be an effective approach to improve wireless communications in such frequency bands with achieving multi-standard purposes.

The associate editor coordinating the review of this manuscript and approving it for publication was Adao Silva.

In fact, the design of compact structures operating simultaneously at sub-6 GHz and mm-Wave bands with same feeding port is very challenging task, due to multiple reasons, particularly: large frequency ratio of mm-Wave to sub-6 GHz bands and considerable electrical length differences between the two bands [2]. Based on this trend, various multi-band antennas operating at both sub-6 GHz and mm-Waves (28 GHz) with different feeding ports have been reported in the literature [2], [3].

The Compact Planar Phased Array for 5G Mobile Terminals described in [1] offers a scan angle above 140^0 with 8 GHz bandwidth. The multilayer beamforming network based on substrate-integrated waveguide seeks to reduce size and provides low profile and high performances, whereas this design is complex with a bulky structure. Comparatively, a simple design is described in [2], which achieves a realized gain of 8 dBi while covering an angle of more than 180° on average. It is also revealed in [3] that wideband end-fire magneto electric dipole antenna element is designed for use in demanding high frequency applications. However, since they only cover the millimeter wave band, these above schemes are not suitable in heterogeneous environments.

Recently, few techniques associated with integrating sub-6 GHz frequencies with 5G millimeter wave array antennas for mobile communications have been presented with some limitations due to compactness, complexity, cost and coverage [4], [5], [6], [7], [8], [9], [10], [11], [12]. In [4], an integrated antenna system for millimeter-wave 5G antennas with Defected Ground Structure is introduced. The design provides a gain value of 10.29 dBi. Two prototypes of dual functional connected slots were provided in [5] and [6]. Because of the lengthy slots in the ground plane and the combined volume necessary for 4G and 5G, both technologies requires a wide antenna profile which makes them unsuitable for portable devices. An integrated antenna system that was developed for both 4G and the next 5G networks is presented in [7]. The two frequency bands cover the range of 1870 MHz to 2530 MHz and mm-Wave at 28 GHz, respectively. The antenna proposed in [8] is comprised of four main compact multi-band loop antennas for sub-6 GHz 5G, as well as four 1 X 8 Yagi phased array antennas for mm-Wave 5G band. Even without considering the influence of dielectric housing, the radiation pattern is altered. On the other hand, the design shown in [9] demonstrated good performance in 5G bands. Nonetheless, it consists of many substructures, which make it complex and less cost effective to manufacture. In addition, the antenna shown in [10] operates in the ranges 700 - 960 MHz, 1710 - 2690 MHz, and 25–30 GHz. This structure requires high accuracy and costly manufacturing process. Contrary to many other types of antenna, millimeter-wave designs may be prototyped using low-cost printed circuit board (PCB) technology [11]. Researchers in [12] present a suggested aperture-sharing integration mechanism for implementing a 3.5/28 GHz antenna capable of achieving peak gains of 7.07 and 11.31 dBi at microwave and millimeter-wave frequencies, respectively. However, the design is quite limited in frequency coverage.

In few words, and regarding drawbacks shown above, novel outcomes should be more explored to meet requirements of both existing and new coming wireless technologies, notably 5G and beyond, in hope of collocating both of them in the best compatible and efficient way avoiding then space limitation challenging issue in portable devices.

In this paper, a handset antenna array is designed to be useful in wireless handheld devices communicating in high and low 5G bands. The proposed antenna system consists of two multiband arrays collocated with one multiband planar antenna. Both cover, simultaneously, sub-6 GHz frequencies (700 MHz /3.5 GHz) and 5G mm-Wave band (28/38 GHz) resulting in quadra-band antenna. To the author's knowledge, very few relevant studies have considered bi-band or tri-band mm-wave but not yet all these four bands in one unique design. One more distinctive key specification of the proposed design is the use of a compact single-layer substrate which guarantees a seamless manufacturing process and effortless integration into various systems. In brief, a well-studied incorporation of diverse multiband structures

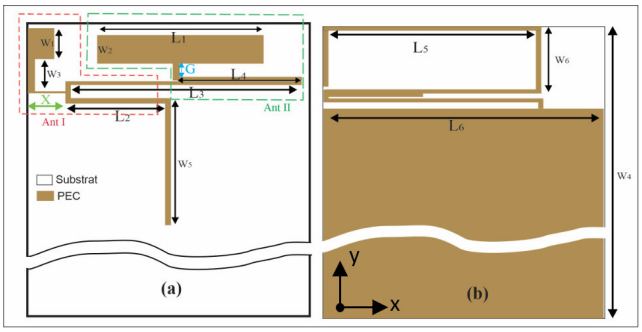

FIGURE 1. Proposed Sub-6 GHz antenna layout (a) top side (b) bottom side.

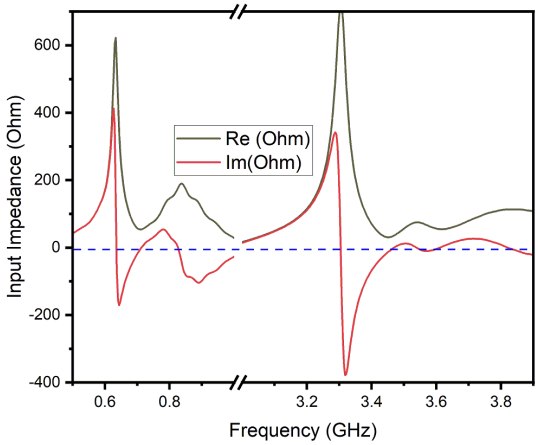

FIGURE 2. Simulated input impedance of Sub-6 GHz Antenna.

allows achieving very promising 5G array features regarding small footprint, multiband operation, radiation coverage and high gain.

Further, the proposed proof-of-concept system design was successfully prototyped, and the observed theoretical and practical performances were quite satisfactory.

II. SUB-6 GHZ ANTENNA DESIGN

The proposed Sub-6 GHz antenna is shown in Fig.1. It is composed of a planar architecture, which is excited by C-shaped strip, operating at 700 MHz frequency band, together with Inverted-U strip coupled to the underground meander line producing 3.5 GHz resonating frequency. The RT Duroid 5880 material (*thickness = 0.508 mm, dielectric permittivity εr = 2.2)* is used as substrate in order to satisfy both mm-Wave and microwave requirements.

The U-monopole is connected to the F-shaped monopole through 50 Ohm microstrip feed-line with narrower microstrip line on the top layer. Via-hole is used to conduct excitation from SMA connector etched in the bottom layer.

For more convenience, the antenna design is divided into two parts: U-shaped monopole as Ant I (red dashed line in Fig.1) and F-shaped strips as Ant II (green dashed line in Fig.1).

Fig. 2 shows the input impedance of both Ant I and Ant II elements. It is seen that Ant I, which is about quarter

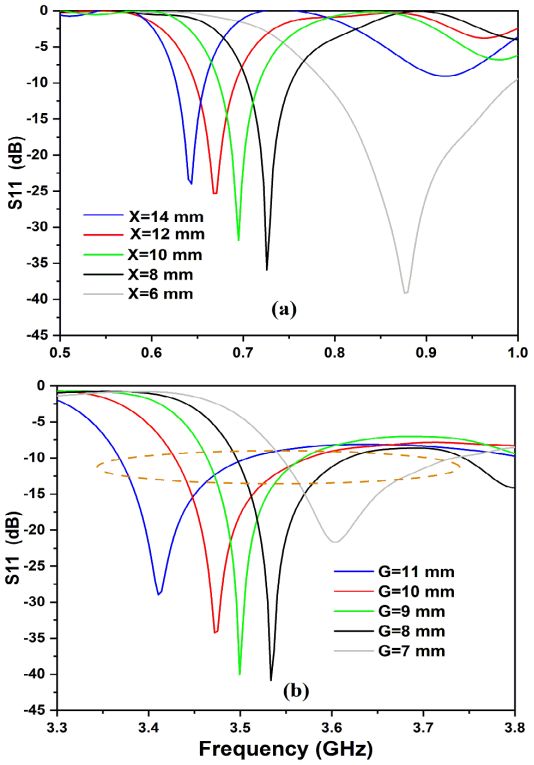

FIGURE 3. Parametric study (a) S11 variation with X tuning (b) S11 variation with G tuning.

TABLE 1. Optimized parameters of sub-6GHz antenna design (in mm).

W1	8.3	*W5*	28.8	*L3*	45.1	*G*	9
W2	8.5	*W6*	13	*L4*	21.2	*X*	10
W3	8.3	*L1*	33	*L5*	43.6	—	—
W4	130	*L2*	15	*L6*	53	—	—

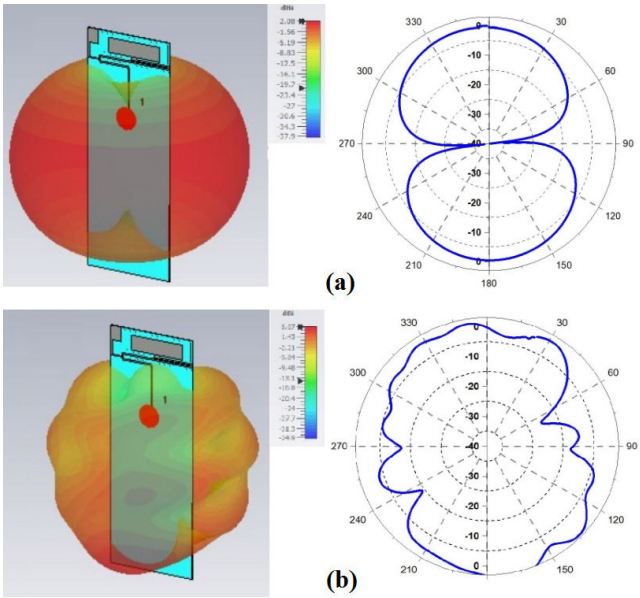

FIGURE 4. 3D and 2D radiation patterns in the E-plane (yz-plane) at (a) 700 MHz and (b) 3.5 GHz.

wavelength at 700 MHz, resonates at around 700 MHz included at sub-6 GHz band, meanwhile Ant II operates at around 3.5 GHz, as expected, due to the addition of the U-shaped monopole. However, the 3.5 GHz impedance bandwidth does not cover all sub-6 GHz standard. Hence, F-shaped planar monopole is inserted to improve the characteristic impedance around 3.5 GHz. The U and F-shaped monopoles improve the impedance matching for the resonant modes, expanding then the impedance bandwidth for low and high bands.

Additionally, parametric analysis, using CST MWS as a simulation tool, is carried out on the important design parameters, namely G and X, to find out the optimized antenna bandwidth. The importance of those parameters is mostly due to the electrical length control through their dimensions and the impedance matching affected by the coupled excitation of the microstrip radiators. This may be further emphasized by analyzing the resonant frequency behaviour which exhibits an inverse relationship with X and G lengths.

Fig. 3 illustrates the corresponding simulated S11 parameters. One can obviously notice that X parameter affects the lower band (700 MHz) while G concerns the higher band (3.5 GHz).

To provide supplementary precision, when the length X is gradually extended from 6 to 14 mm, the reflection coefficient exhibits a noticeable proportional shift towards lower frequencies. This linear shift observation suggests that the C-shaped strip associated with 10mm length of X operates as a quarter-wavelength ($\lambda/4$) resonator at 700MHz. Similarly, the Inverted-U strip extended with 9mm length of G, generates almost a quarter-wavelength monopole behaviour at 3.5GHz. Consequently, the sub-6 GHz design comportment can be summarized as a combination of coupled double-monopoles co-designed for working together at different frequencies, providing a dual band feature.

Further, all optimized parameters of such design are detailed in Table 1.

Radiation pattern is also studied in both frequencies 700MHz and 3.5GHz. 3D and 2D CST simulations, shown in Fig.4, confirm the omnidirectional radiation feature of the proposed antenna in sub-6GHz band.

III. 28/38 GHZ MM-WAVE ANTENNA ARRAY STRUCTURE

In this section, the main goal is to develop a dual band and high gain antenna array for use in mm-Wave band, namely 28 and 38GHz. Figure 5 depicts the layout of the proposed design, composed of four-pole array and a microstrip power divider. This configuration makes it symmetrically invertible around the x-axis. Details of the structure dimensions are listed in Table 2.

Each element of the array looks like S-dipole, consisting of two top arms coupled to bottom ones through grounded-rectangular slots inserted in the radiating parts (Fig.5). The operation principle of each single element is quasi-similar to that of a conventional dipole. The array is fed with parallel

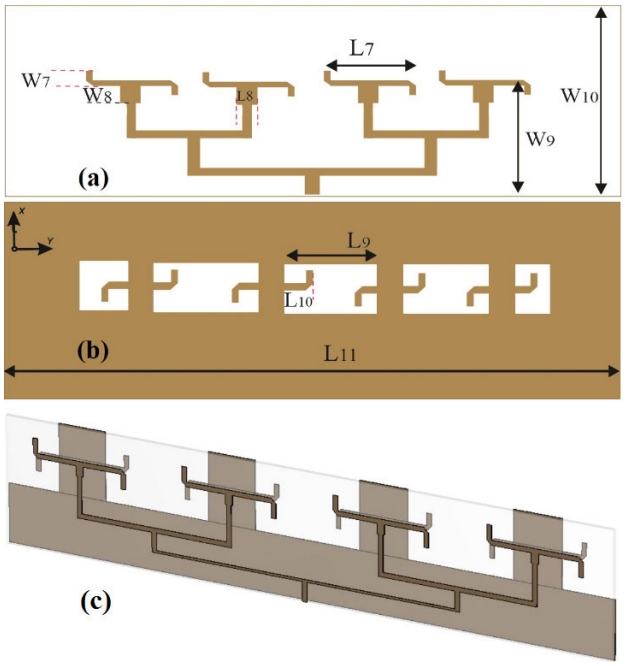

FIGURE 5. Proposed 28/38 GHz mm-Wave antenna array (a) top side (b) bottom side (c) 3D view.

TABLE 2. Optimized parameters of the mm-Wave structure (in mm).

W7	2	*L7*	10.5	*L11*	64
W8	1.1	*L8*	0.8	—	—
W9	9.9	*L9*	11	—	—
W10	13	*L10*	3.8	—	—

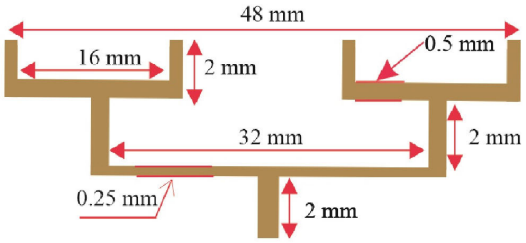

FIGURE 6. Power divider layout.

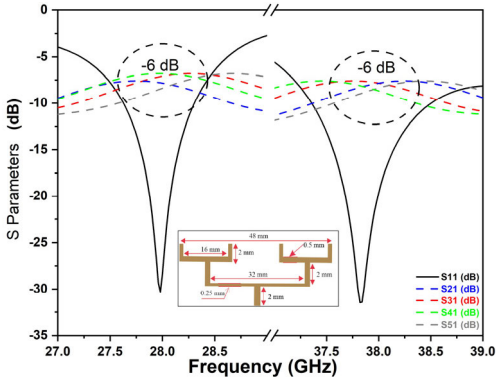

FIGURE 7. Simulated S-Parameters of the power divider.

in-phase signals using one-to-four-microstrip power divider, as seen in Fig.6.

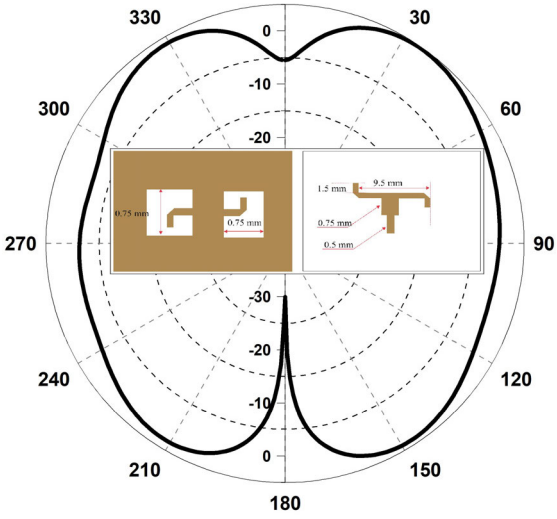

FIGURE 8. Radiation pattern (xy-plane) of one element composing the mm-Wave array.

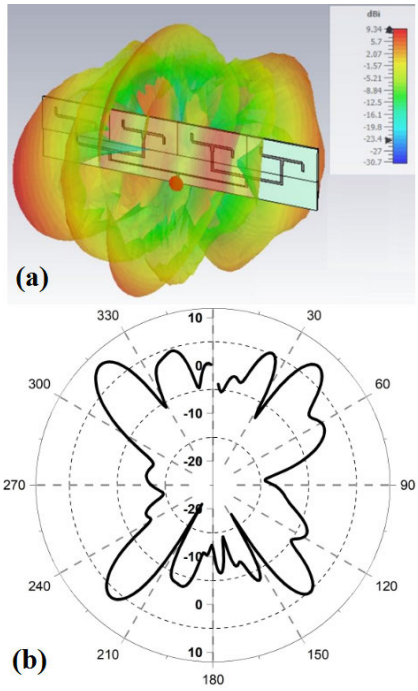

FIGURE 9. Simulated radiation pattern of the proposed mm-Wave array at 28GHz (a) 3D pattern (b) pattern at yz-plane.

Simulation results, shown in Fig.7, demonstrate that the proposed power divider is well matched with slight losses in both targeted frequencies 28 and 38 GHz, as the reflection coefficient $|S_{11}| \approx -30$ dB, and the transmission coefficients $|S_{ij}|$ are around -6 dB$\approx 10 \log (1/4)$.

Further, it is obviously noticed, from Fig.8, that the pole's radiation pattern is quite omnidirectional, which confirms the operation likeness with conventional dipole.

Moreover, the four poles are intentionally aligned along the y-axis in order to produce directional radiation pattern with high gain, as well (Fig.9), achieved by constructive radiation

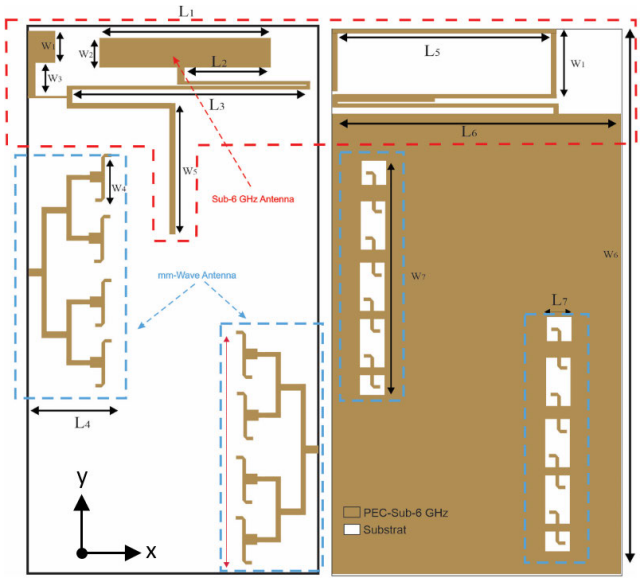

FIGURE 10. Proposed handset antenna array.

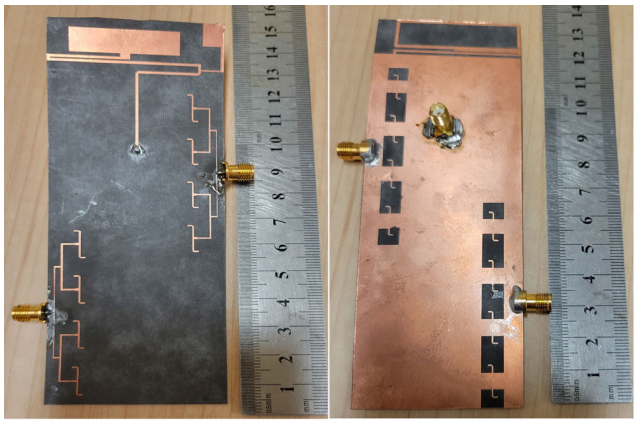

FIGURE 11. Fabricated 5G handset antenna.

FIGURE 12. Radiation pattern measurement testbed.

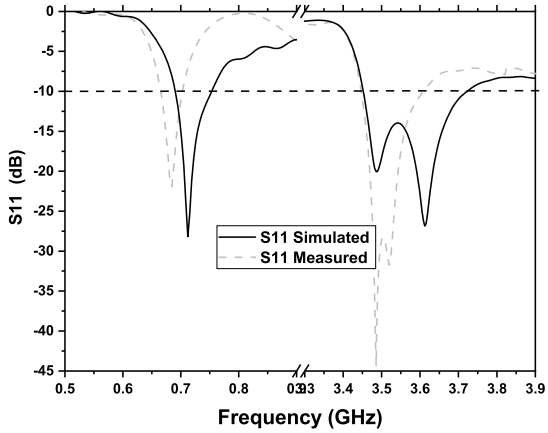

FIGURE 13. Simulated and Measured reflection coefficient S11 of the proposed antenna, in sub-6GHz.

combination through the use of in-phase one to four power divider.

IV. COLLOCATION APPROACH OF SUB-6 GHZ ANTENNA WITH 28/38 GHZ MM-WAVE ARRAY STRUCTURE

This section is dedicated to address the final design steps including the combination methodology, within an assembled compact structure, of the previous designs discussed in sections II and III.

Fig.10. depicts the final layout design incorporating two similar mm-Wave antenna arrays, located in the opposite edges of the structure. Both are collocated with sub-6 GHz antenna with same optimized parameters, as listed above in Tables 1 and 2. This intent collocation procedure provides interesting specifications, regarding the good impedance matching in all targeted frequencies, with less electromagnetic coupling and well established radiation patterns in both sub-6GHz and mm-Wave bands. Detailed results are demonstrated bellow.

The manufactured handset array is shown in Fig. 11. The prototype, with overall size of about $53 \times 130 \times 0.508\text{mm}^3$, is fabricated using Rogers RT Duroid 5880 substrate. S-Parameters were measured using Anritsu MS4647A network analyzer and radiation characteristics have been studied in anechoic chamber (Fig.12).

Fig. 13 shows the measured and simulated reflection coefficients of the proposed compact antenna in sub-6GHz. Despite some minor discrepancies between the simulated and measured findings, they are still comparable. Hence, obtained results confirm that the design is capable of operating at frequencies as low as 700 MHz and as high as 3.55GHz, with sufficient bandwidths of about 160MHz and 250MHz, respectively.

In Fig.14 are compared the computed and measured S-parameters of the antenna array in 5G mm-Wave band (28 and 38 GHz).

It is seen that satisfactory -10 dB impedance matching is obtained in both 28 and 38 GHz bands. We note also that important antenna isolation is achieved since S21 parameter is bellow −40 dB in the entire bands.

Although the resonance frequency is slightly moved to higher frequency, the observed S-parameter characteristics

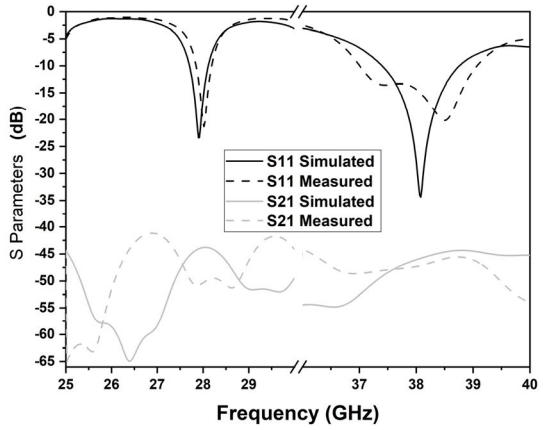

FIGURE 14. Simulated and measured S-Parameters of the proposed antenna in mm-Wave.

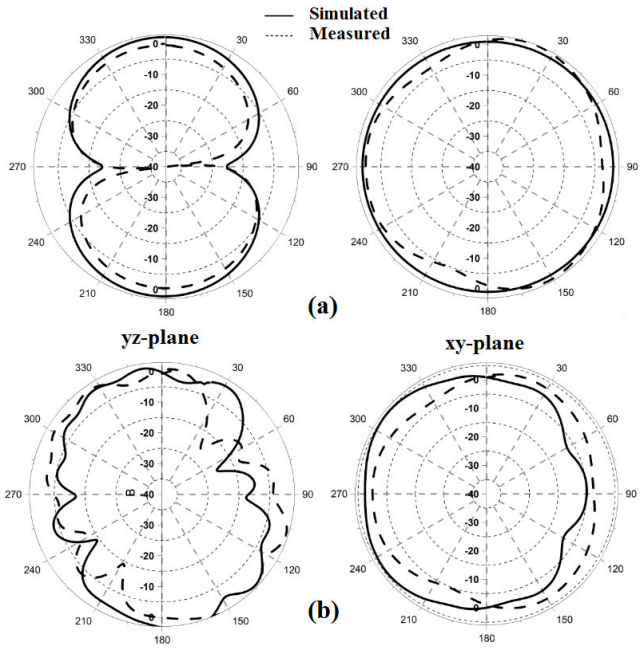

FIGURE 15. Simulated and measured radiation patterns in both E-plane (yz-plane) and H-plane (xy-plane) at (a) 700 MHz (b) 3.5 GHz.

are extremely similar to the simulated ones. Compared to 3.5 GHz band, mm-Wave results show higher likeness between measurement and simulation.

Fig.15 illustrates the simulated and measured radiation patterns at sub-6 GHz in both azimuthal and elevation planes. The pattern looks well omnidirectional in the lower band (700MHz), which confirms that predicted pattern is not much disturbed by the presence of the millimeter-wave structure. However, it is slightly tilted in the upper band (3.5GHz) and the pattern is somehow altered in some directions. Still the radiation characteristics are interesting and useful in the sub-6GHz band. Moreover, consistent agreement is noticed between simulation and measurement results.

Besides, Fig.16 depicts the simulated and measured radiation appearance of the array at 28 and 38 GHz. Acceptable alignment between simulated and measured results is obtained.

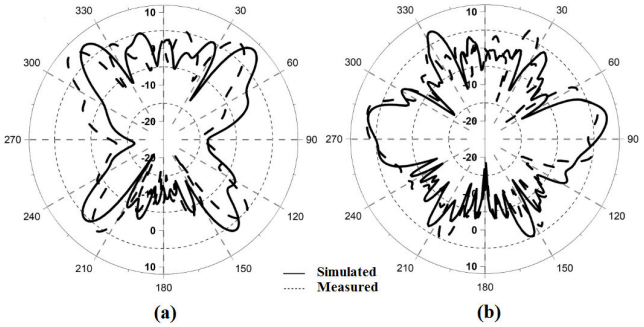

FIGURE 16. Simulated and measured radiation pattern in E-plane (yz-plane) at (a) 28GHz (b) 38 GHz.

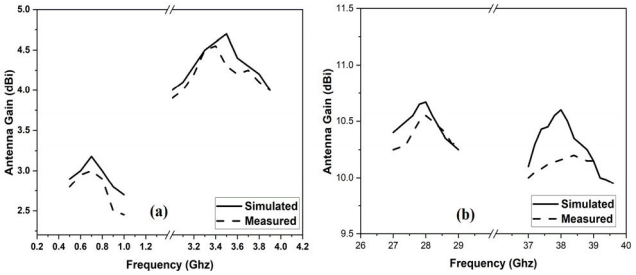

FIGURE 17. Simulated and measured peak gain at (a) sub- 6GHz band (b) mm-Wave bands.

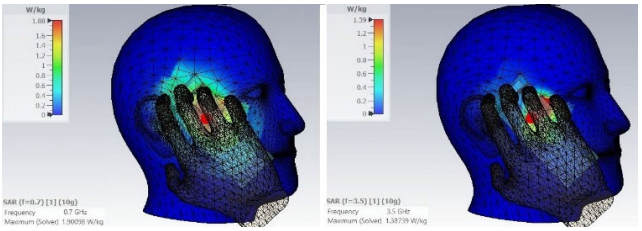

FIGURE 18. 10g average SAR distributions of the proposed Antenna system at 700 MHz (left figure) and 3.5 GHz (right figure).

The peak gain of the proposed design is simulated and measured, as well. Obtained results are displayed in Fig 17. One can notice that high gain is achieved as it reaches 4.6 dBi at 3.5 GHz and almost 10.5 dBi at 28GHz.

To be closer to the real-world, beside user safety which is of utmost priority, as stipulated in various international organizations, regarding human exposure risk [15], [16], the influence of head/hand phantoms is deeply studied and analyzed through simulation model in CST Microwave Studio, as illustrated in Fig. 18. The modeling of the proposed antennas focuses on analyzing Specific Absorption Rate (SAR) in the sub-6GHz range and Power Density (PD) in the mm-Wave frequency band.

In Fig. 18 is demonstrated the SAR value at sub-6 GHz using 10g standard. The obtained maximum SAR values are 1.9 W/kg and 1.38 W/kg at 700 MHz and 3.5 GHz, respectively. Similarly, the power density peak values amount to 160 W/m^2 at 28 GHz and 180 W/m^2 at 38 GHz. We note that both SAR and PD values satisfy the current International Commission on Non-Ionizing Radiation Protection (ICNIRP) limits [16].

TABLE 3. Comparative study.

Refs	*Antenna size (mm^3)*	*Microwave center* ***Frequency band*** *(GHz)*	*mm-wave center* ***Frequency band*** *(GHz)*	*Efficiency (%) (sub-6Ghz/mm-wave)*	*Max Gain(low Fre/High Fre) (dBi)*	*Process Type*
[7]	70 x 60 x 0.381	2.4	28	45-70/60-90	4.5/12.5	Single layer PCB
[9]	162.6 x 77.7x 0.508	3.5	28	93.6/96	2.3/7.7	Single layer PCB
[11]	33.9 x 43 x 0.254	3.5	28	-	7.07/11.31	Single layer PCB
[13]	147 x 72 x 0.25	3.5	28	75/85	2.5/8	Metal rim, Multi-layer
[14]	131 x 77 x 0.305	0.8/2.2	26	40/-	1.5/10.4	Single layer PCB
This work	**130 x 53 x 0.508**	**0.7/3.5**	**28/38**	**55-60/88-90**	**4.6/10.5**	**Single layer PCB**

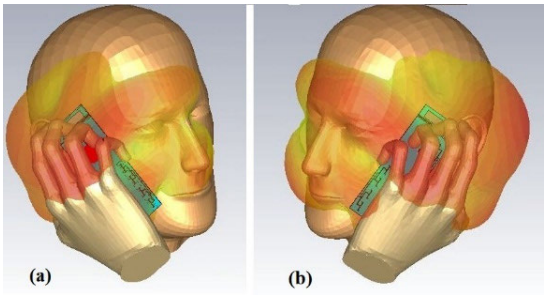

FIGURE 19. Simulated 3-D radiation pattern (a) right hand (b) left hand.

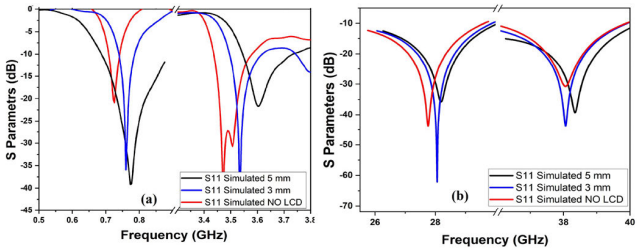

FIGURE 20. LCD Effect on the proposed design with different spacing between the LCD and the ground plane at (a) sub-6 GHz band (b) mm-wave band.

Further, it is shown from Fig.19 that antenna array 1, situated in close proximity to the head/hand phantom, experiences substantial effects, whereas the influence on antenna array 2, located farther from the phantoms, is comparatively subdued. Antenna array 1 demonstrates robust radiation efficiency, reaching up to 60%, particularly when the right hand is in use, while antenna array 2 exhibits commendable performance under left-hand utilization. The observed distinctions may be attributed to the notable electromagnetic field absorption by the hand/head phantom and the distinctive positioning of the antenna array in relation to the phantom.

Besides, the impact of incorporating a Liquid Crystal Display (LCD) is examined through CST MWS simulations. The LCD module consists of two parts: the LCD panel (glass with a relative permittivity of 7 and a loss tangent of 0.02, adhered to the LCD shield) and LCD shield (stainless steel adhered to the ground plane). The LCD, measuring 135 mm × 75 mm × 0.5 mm, is positioned beneath the ground plane and treated as a perfect electric conductor (PEC). The investigation includes simulations of the reflection coefficient in presence of LCD device with gap distance of 3 mm and 5 mm from the ground plane. Fig. 20 illustrates the influence of the LCD module on the antenna array, which is seen as a slight shift of resonant frequencies to higher bands in both microwave and mm-wave frequency ranges. This slight influence can be easily adjusted by simply tuning the structure parameters, namely, the dimensions of the radiators.

V. COMPARISON WITH RELATED WORKS

Finally, a comparative study is drawn in Table 3, in order to highlight clearly our achievement compared to some relevant literature results. Hence, the proposed design undergoes evaluation based on its capacity to integrate both mm-wave and sub-6 GHz frequencies within a unified structure, which is considered a pioneering area, with limited available literature on reported designs. Table 3 unequivocally illustrates the unique feature of the suggested design, encompassing all 5G frequency bands within a singular structure, distinguishing it from previous designs. Notably, the integration of 5G and sub-6GHz is achieved in reference [14], albeit with a compact form factor. However, this integration only covers the 26 GHz band within the mm-wave spectrum. Despite its high efficiency, the antenna in [9] operates solely within the frequency range of 3.5 GHz and 28 GHz. All other antenna designs, including [9], [13], and [14], span various frequency ranges excluding mm-Wave, showcasing variations in both achieved gain, efficiency and process type. In conclusion, it is demonstrated the effective advancement offered by the proposed structure as innovative approach to integrating antennas for forthcoming 5G technologies within a single framework, featured mainly by smallest dimensions, important gain and exclusively Quadra-band frequency coverage.

VI. CONCLUSION

Combined mm-Wave and microwave antenna design for wireless handheld devices and mobile terminals is proposed in this study. Both antennas share the same volume of a compact PCB layer. The handset antenna comprises two millimeter wave arrays and one sub-6 GHz structure, providing exceptionally a very large operating frequency ratio with important average gain of around 10.5dBi and 4.6dBi, respectively. Conducted simulation and measurement show good agreement in terms of impedance bandwidth, gain and radiation pattern. Further, the design meets the MIMO antenna

system requirements, along with other advantageous features, such as: low profile, low cost, simple fabrication process and ease of practical integration with other digital circuits. Consequently, the proposed structure is a reliable promising candidate for wireless devices operating in 5G technology. Moreover, this compact multiband antenna is highly recommended for some radiofrequency terminal applications involved in severe situations with important constraints, such those found in underground mining environments characterized by deep power attenuation due to the non-line of site (NLOS) wave propagation. Hence, it can be integrated into miner's handset systems and communication equipment, as well as can be installed in autonomous machinery for future smart mines.

In this same context, future works may focus on the detailed exploration of the handset antenna performance under various real-world conditions.

REFERENCES

[1] I. Syrytsin, S. Zhang, G. F. Pedersen, and A. S. Morris, "Compact quad-mode planar phased array with wideband for 5G mobile terminals," *IEEE Trans. Antennas Propag.*, vol. 66, no. 9, pp. 4648–4657, Sep. 2018, doi: 10.1109/TAP.2018.2842303.

[2] C. Di Paola, S. Zhang, K. Zhao, Z. Ying, T. Bolin, and G. F. Pedersen, "Wideband beam-switchable 28 GHz quasi-Yagi array for mobile devices," *IEEE Trans. Antennas Propag.*, vol. 67, no. 11, pp. 6870–6882, Nov. 2019, doi: 10.1109/TAP.2019.2925189.

[3] J. Zeng and K.-M. Luk, "Wideband millimeter-wave end-fire magnetoelectric dipole antenna with microstrip-line feed," *IEEE Trans. Antennas Propag.*, vol. 68, no. 4, pp. 2658–2665, Apr. 2020, doi: 10.1109/TAP.2019.2957089.

[4] Y. Liu, Y. Li, L. Ge, J. Wang, and B. Ai, "A compact hepta-band mode-composite antenna for sub (6, 28, and 38) GHz applications," *IEEE Trans. Antennas Propag.*, vol. 68, no. 4, pp. 2593–2602, Apr. 2020, doi: 10.1109/TAP.2019.2955206.

[5] M. Ikram, N. Nguyen-Trong, and A. M. Abbosh, "Common-aperture sub-6 GHz and millimeter-wave 5G antenna system," *IEEE Access*, vol. 8, pp. 199415–199423, 2020, doi: 10.1109/ACCESS.2020.3034887.

[6] M. Ikram, N. Nguyen-Trong, and A. M. Abbosh, "Realization of a tapered slot array as both decoupling and radiating structure for 4G/5G wireless devices," *IEEE Access*, vol. 7, pp. 159112–159118, 2019, doi: 10.1109/ACCESS.2019.2950660.

[7] M. Ikram, E. A. Abbas, N. Nguyen-Trong, K. H. Sayidmarie, and A. Abbosh, "Integrated frequency-reconfigurable slot antenna and connected slot antenna array for 4G and 5G mobile handsets," *IEEE Trans. Antennas Propag.*, vol. 67, no. 12, pp. 7225–7233, Dec. 2019, doi: 10.1109/TAP.2019.2930119.

[8] M. Ko, H. Lee, and J. Choi, "Planar LTE/sub-6 GHz 5G MIMO antenna integrated with mmWave 5G beamforming phased array antennas for V2X applications," *IET Microw., Antennas Propag.*, vol. 14, no. 11, pp. 1283–1295, Sep. 2020, doi: 10.1049/iet-map.2019.0849.

[9] M. Zada, I. A. Shah, and H. Yoo, "Integration of sub-6-GHz and mm-wave bands with a large frequency ratio for future 5G MIMO applications," *IEEE Access*, vol. 9, pp. 11241–11251, 2021, doi: 10.1109/ACCESS.2021.3051066.

[10] J. Kurvinen, H. Kähkönen, A. Lehtovuori, J. Ala-Laurinaho, and V. Viikari, "Co-designed mm-wave and LTE handset antennas," *IEEE Trans. Antennas Propag.*, vol. 67, no. 3, pp. 1545–1553, Mar. 2019, doi: 10.1109/TAP.2018.2888823.

[11] M. L. Seddiki, S. E. Hadji, and M. Nedil, "A triple-band antenna for indoor 5G applications," in *Proc. IEEE Int. Symp. Antennas Propag. USNC-URSI Radio Sci. Meeting (AP-S/URSI)*, Jul. 2022, pp. 1816–1817.

[12] J. Lan, Z. Yu, J. Zhou, and W. Hong, "An aperture-sharing array for (3.5, 28) GHz terminals with steerable beam in millimeter-wave band," *IEEE Trans. Antennas Propag.*, vol. 68, no. 5, pp. 4114–4119, May 2020, doi: 10.1109/TAP.2019.2948706.

[13] R. S. Malfajani, F. B. Ashraf, and M. S. Sharawi, "A 5G enabled shared-aperture, dual-band, in-rim antenna system for wireless handsets," *IEEE Open J. Antennas Propag.*, vol. 3, pp. 1013–1024, 2022.

[14] Y. Wang and F. Xu, "Shared-aperture 4G LTE and 5G mm-wave antenna in mobile phones with enhanced mm-wave radiation in the display direction," *IEEE Trans. Antennas Propag.*, vol. 71, no. 6, pp. 4772–4782, Jun. 2023.

[15] K. Zhao, Z. Ying, and S. He, "EMF exposure study concerning mmWave phased array in mobile devices for 5G communication," *IEEE Antennas Wireless Propag. Lett.*, vol. 15, pp. 1132–1135, 2016.

[16] International Commission on Non-Ionizing Radiation Protection, "Guidelines for limiting exposure to electromagnetic fields (100 kHz to 300 GHz)," *Health Phys.*, vol. 118, no. 5, pp. 483–524, May 2020, doi: 10.1097/HP.0000000000001210.

MOHAMED LAMINE SEDDIKI received the Engineering degree in telecommunication from the University of Blida, Algeria, in 2012, and the M.Sc. degree from Université du Québec en Abitibi-Témiscamingue (UQAT), in 2017, where he is currently pursuing the Ph.D. degree. He has been a Research Assistant with UQAT, since 2018. His research interests include microwave components, microwave reconfigurable circuits, and MIMO antenna.

MOURAD NEDIL (Senior Member, IEEE) received the Dipl.-Ing. degree from the University of Algiers, Algiers, Algeria, in 1996, the D.E.A (M.S.) degree from the University of Marne la Vallée, Marne la Vallée, France, in 2000, and the Ph.D. degree from Institut National de la Recherche Scientifique (INRS-EMT), Université de Québec, Montreal, QC, Canada, in 2006. He has completed a Postdoctoral Fellowship with the RF Communications Systems Group, INRS-EMT, from 2006 to 2008. In 2008, he joined the Engineering School Department, Université du Québec en Abitibi-Témiscamingue, Rouyn-Noranda, QC, where he is currently an Associate Professor. His current research interests include antennas, multiple-input and multiple-output radio-wave propagation, and microwave devices.

SOUFIANE TEBACHE received the Engineering degree in electronics and telecommunications from the Polytechnic School of Algeria, in 2009, the Magister degree in signals and communications, in 2013, and the Ph.D. degree (summa cum laude) from Ecole Nationale Polytechnique (ENP), Algeria, in 2021. His research interests include antenna and RF system design, MIMO, and wireless communications.

SAIF EDDINE HADJI received the Dipl.-Ing. degree from the Military Polytechnic School, Algiers, Algeria, in 2009, and the M.Sc. degree from the University of Technology Malaysia (UTM), Johor Bahru, Malaysia, in 2016, where he is currently pursuing the Ph.D. degree. He is also doing research with Université du Québec en Abitibi-Témiscamingue (UQAT). His current research interests include wireless communication in underground mines, mmWave, and massive MIMO systems.